Prediction of ozone effects on net ecosystem production of Norway spruce forest

Stanislav Juráň [1],
Magda Edwards-Jonášová [1],
Pavel Cudlín [1],
Miloš Zapletal [1-2],
Ladislav Šigut [1],
John Grace [1-3],
Otmar Urban [1]

Future ground-level concentrations of phytotoxic ozone are projected to grow in the Northern Hemisphere, at a rate depending on emission scenarios. We explored the likely changes in net ecosystem production (NEP) due to the increasing concentration of tropospheric ozone by applying a Generalized Additive Mixed Model based on measurements of ozone concentration ($[O_3]$) and stomatal ozone flux (FsO_3), at a mountainous Norway spruce forest in the Czech Republic, Central Europe. A dataset covering the growing period (May-August 2009) was examined in this case study. A predictive model based on FsO_3 was found to be marginally more accurate than a model using $[O_3]$ alone for prediction of the course of NEP when compared to NEP measured by the eddy covariance technique. Both higher $[O_3]$ and FsO_3 were found to reduce NEP. NEP simulated at low, pre-industrial FsO_3 (0.5 nmol m^{-2} s^{-1}) was higher by 24.8% as compared to NEP assessed at current rates of FsO_3 (8.32 nmol m^{-2} s^{-1}). However, NEP simulated at high FsO_3 (17 nmol m^{-2} s^{-1}), likely in the future, was reduced by 14.1% as compared to NEP values at current FsO_3. The interaction between environmental factors and stomatal conductance is discussed in this paper.

Keywords: Carbon, CO$_2$ Assimilation, Model, Stomatal Ozone Flux

Introduction

Tropospheric ozone (O$_3$), a common phytotoxic secondary air pollutant, reduces growth and carbon sequestration potential of terrestrial vegetation (Subramanian et al. 2015). Despite the limited nature of observations in the 19th century, ozone concentrations are reported to have undergone an increase from the base level of 10-15 ppbv in the pre-industrial era (Royal Society 2008) to current concentrations of 35-45 ppbv in large parts of the industrialised world, with an average rate of increase of about 5 ppbv per decade in the Northern Hemisphere (Cooper et al. 2014). It is estimated that the long-term increase in tropospheric O$_3$ concentration ($[O_3]$) has led to a substantial reduction in carbon uptake, as compared to the pre-industrial era (Cooper et al. 2014). While daily maxima of $[O_3]$ may now be decreasing, annual mean $[O_3]$ has been increasing over the last decade (Paoletti et al. 2014).

Recent studies at different hierarchical levels have shown that O$_3$ reduces photosynthetic carbon assimilation and changes carbon allocation in trees and forest ecosystems (Wittig et al. 2009, Sicard et al. 2016). It has been demonstrated that O$_3$ alters the source-sink balance in plants, resulting initially in carbon retention in shoots and decreased carbon allocation in below ground biomass (reviewed by Andersen 2003). Rising $[O_3]$ thus has a significant potential to affect terrestrial carbon sinks and regional hydrology (Wittig et al. 2009, Sun et al. 2012). Most of the studies were, however, conducted on seedlings or juvenile trees and the assessment of the O$_3$ impact on mature trees is still at an early stage (Zapletal et al. 2011, 2012, Fares et al. 2013). Accordingly, there is an increasing demand for long-term studies conducted under natural, ecologically relevant conditions (Fares et al. 2018).

To quantify the detrimental dose of O$_3$ on vegetation, several indices have been established: AOT40 (accumulated exposure over a threshold of 40 ppbv) and POD$_y$ (accumulated ozone flux above a given flux threshold y [nmol m^{-2} s^{-1}]). Critical levels are assessed as an estimation above which detrimental effects may occur. The magnitude of both indices depends on species, environmental conditions and the capacity of plant defence mechanisms (Musselman & Massman 1998). Verryckt et al. (2017) reported no impact of ambient $[O_3]$ on carbon uptake in sub-urban mature pine forest in the vicinity of Antwerp city, Belgium, although the critical levels for both AOT40 and POD$_1$ indices were exceeded. Similarly, an ambient $[O_3]$ of 50 ppbv (mean value) had no effect on leaf injury in black cherry and red maple seedlings during the period of April-August. While visible symptoms of foliar injury were observed under doubled $[O_3]$ (Samuelson 1994), no visible damages of leaves nor reduction in CO$_2$ uptake were observed in poplar plantation at a cumulative stomatal O$_3$ uptake of 25-27 mmol m^{-2} (Zona et al. 2014).

Contrary to these findings, growth decreased by 6.6% in Swiss forests during the period 1991-2011, particularly in European beech and Norway spruce (Braun et al. 2014), and this decline was ascribed to rising $[O_3]$. Similarly, Gross Primary Production (GPP) was reduced by 4-8% on average in eastern US vegetation peaking up to 11-

17% during an occurrence of high O_3 episodes (Yue & Unger 2014). Only a limited effect of O_3 on photosynthesis was observed in the broad-leaved Harvard forest (Yue et al. 2016). Norway spruce (*Picea abies* Karst.), a wide-spread tree species of the temperate zone and especially Central Europe, has previously been described as an ozone sensitive tree species (Zapletal et al. 2011). Subramanian et al. (2015), among others, reported a decrease in photosynthetic carbon assimilation of 4.3-15.5% due to an exposure to high $[O_3]$. As most studies were conducted on seedlings under controlled conditions (Skärby et al. 1998), estimation and quantification of O_3 effects at the ecosystem scale under field conditions received only limited attention.

In the present study, we attempted to quantify the effect of O_3 on Net Ecosystem Production (NEP), defined as the difference between ecosystem-level photosynthetic uptake of CO_2 and ecosystem respiratory loss of CO_2. Our attention was focussed on a mountainous spruce forest in the Czech Republic. NEP values measured by eddy covariance were compared to those estimated by the Generalized Additive Mixed Model (GAMM). We tested the efficacy of $[O_3]$- and stomatal ozone flux (FsO_3)-based GAMM models to predict diurnal and seasonal changes in NEP. To determine O_3 effects, NEP was calculated in a simulation model at low, pre-industrial $[O_3]$ (12 ppbv) and FsO_3 (0.5 nmol m^{-2} s^{-1}) as well as at high $[O_3]$ (80 ppbv) and FsO_3 (17 nmol m^{-2} s^{-1}) expected at the end of the century (Meehl et al. 2007, Cooper et al. 2014). We hypothesized that tropospheric ozone reduces NEP in Norway spruce forest. To test this hypothesis, we investigated effects of $[O_3]$ and FsO_3 on NEP during four representative days of the main growing season differing in degree of cloudiness and thus in daily maxima of solar radiation intensity, air temperature, and vapour pressure de-

ficit. These representative days also covered seasonal course in NEP and enabled thus to model effects of $[O_3]$ and FsO_3 on NEP throughout the growing season (May-August).

Material and methods

Site description

The forest stand is located at the Bílý Kříž experimental research site within the Beskydy Mountains in the north-east of the Czech Republic (49° 30′ N, 18° 32′ E; 875-908 m a.s.l.). The experimental research site forms part of several international research networks and infrastructures: CzeCOS (Czech Carbon Observation System), ICOS (Integrated Carbon Observation System), and AnaEE (Analysis and Experimentation on Ecosystems). The forest stand (99% *Picea abies* and 1% *Abies alba*) had been established in 1981 by row planting of 4-year-old Norway spruce seedlings. Mean stand slope is 13° and exposure is to the south. In 2009, the year of investigation, the average stand height was 13 m, tree density was 1420 trees ha^{-1}, average stem diameter at breast height was 15.9 cm, and leaf area index based on hemispherical photographs was 9.6 m^2 m^{-2}.

The area has a moderately cool (mean air temperature 6.8 °C) and humid (mean relative air humidity 84%) climate with high annual precipitation (mean annual precipitation 1318 mm; years 1998-2009). Due to an even distribution of precipitation over the year, values of soil volumetric water content remain high during the growing season ranging between 20 and 30% irrespective of sky conditions. The region is characterized by low concentrations of nitrogen oxides (below 10 ppbv) and high $[O_3]$, exceeding 80 ppbv during summer months (Zapletal et al. 2011). Diurnal courses of selected environmental variables, including diurnal changes in $[O_3]$, for representative

days are shown at Fig. 1.

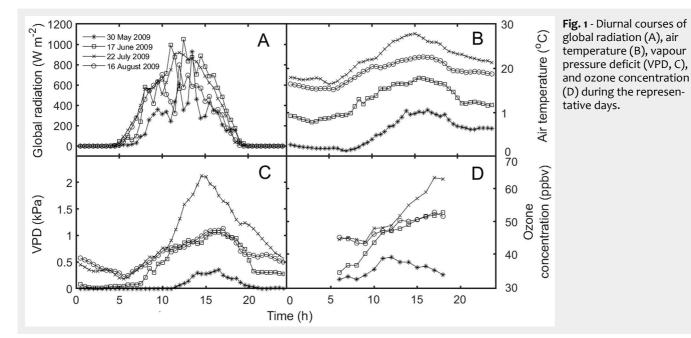### Measurement of environmental variables

The measurements were conducted from May 28 to September 30, 2009, during the daytime (06:00-18:00 GMT+1) to cover the periods characterized by well-developed turbulent mixing. A meteorological mast (36 m tall) situated within the studied stand was equipped with a set of meteorological sensors and an eddy covariance system. Air temperature (Tair) and relative air humidity (RH) were measured by an EMS33 Rotro® sensor (EMS, Brno, Czech Republic). These variables were used to calculate the values of vapour pressure deficit (VPD) according to the formula (eqn. 1):

$$VPD = \frac{100 - RH}{100} \cdot 610.7^{\frac{7.5\,T\,air}{237.3+T\,air}} \quad (1)$$

The barometers PTB110® (Vaisala, Vantaa, Finland) and SPA 511 B5UB® (CRESSTO, Roznov pod Radhostem, Czech Republic) were used to measure air pressure. Global radiation (GR) was measured by a pyranometer CM6B® (Kipp & Zonen, Delft, Netherlands). The 2D ultrasonic anemometer 50.5 (Met One Instruments, Grants Pass, OR, USA) was used for the measurement of horizontal wind speed. All standard meteorological measurements were made on a vertical profile at heights of 2, 7, 10, 11.5, 12.25, 13, 13.5, 14, 15, 17, 21, and 28 m above the soil surface. The signals from all sensors were recorded every 30 s and stored as half-hourly averages using a data logger (Delta-T®, Burwell, Cambridgeshire, UK). In addition, precipitation was recorded by a precipitation gauge 386C (Met One Instruments, Grants Pass, OR, USA).

Estimation of CO_2 and O_3 fluxes

An eddy covariance system was used to measure the CO_2 and water vapour fluxes between the forest stand and the atmos-

Fig. 1 - Diurnal courses of global radiation (A), air temperature (B), vapour pressure deficit (VPD, C), and ozone concentration (D) during the representative days.

phere. The system consisted of a Gill R3® ultrasonic anemometer (Gill Instruments, Hampshire, UK) and an enclosed-path infrared gas analyser LI-7200® (LI-COR Biosciences, Lincoln, NE, USA) placed 18 m above the soil surface. The post-processing of high frequency data (20 Hz) was performed by EddyPro® software (LI-COR Biosciences, USA) according to recent recommendations (Aubinet et al. 2012) and expressed as half-hourly estimates. This procedure included spike removal and quality check of the raw signals, rotation of wind velocity components into the planar fit coordinate system, and spectral corrections of computed fluxes. The missing and excluded data, based on the quality checking scheme, were gap-filled by the marginal distribution sampling method according to Reichstein et al. (2005). Sign convention was adopted as follows: positive values represent CO_2 uptake, thus enabling convenient modelling of NEP as a general non-rectangular hyperbolic function of incident GR (Urban et al. 2012).

[O_3] was measured at 5, 15, and 25 m above the soil surface using slow-response O_3 analysers $O_3$41M® (Environment S.A., Poissy, France). The signals from all O_3 analysers were recorded as half-hourly averages.

Stomatal ozone flux (FsO_3) to the Norway spruce forest was calculated according to Cieslik (2004 – eqn. 2)

$$FsO_3 = \frac{R_c}{[R_a(z) + R_b + R_c] R_{sto}} \cdot c(z) \qquad (2)$$

where $c(z)$ is O_3 concentration at a height z = 2 m above the canopy, R_a is the aerodynamic resistance for the turbulent layer, R_b is the laminar layer resistance for the quasi-laminar layer, and R_c is the surface or canopy resistance of the receptor. R_c was calculated as (eqn. 3):

$$R_c = \left(\frac{LAI}{R_{sto}} + \frac{SAI}{R_{ext}} + \frac{1}{R_{inc} + R_{soil}} \right)^{-1} \qquad (3)$$

where R_{sto} is the land-cover specific needle stomatal resistance to O_3 uptake, R_{ext} is the resistance of the external plant parts to uptake or destruction of O_3, R_{inc} is the land-cover specific in-canopy aerodynamic resistance to transport of O_3 towards the soil and lower parts of the canopy, R_{soil} is the soil resistance to destruction or absorption of O_3 at the ground surface, LAI is leaf area index, and SAI is a surface area index set equal to LAI in the growing season.

Stomatal resistance component R_{sto} was calculated as described in Emberson et al. (2000 – eqn. 4):

$$R_{sto} = g_{max} \cdot g_{phen} \cdot$$
$$\cdot max \left\{ g_{min}, \left(g_{light} \cdot g_{temp} \cdot g_{VPD} \cdot g_{SWP} \right) \right\}^{-1} \qquad (4)$$

where g_{max} is the average maximum stomatal conductance of *Picea abies* to ozone (nmol O_3 m^2 s^{-1}) expressed on total needle surface area. The parameters g_{phen}, g_{light}, g_{temp}, g_{VPD}, and g_{SWP} are expressed in relative terms between 0 and 1, and represent the

Tab. 1 - Meteorological variables of the period May 28-September 30, 2009. [O_3]: ozone concentration; (FsO_3): stomatal ozone flux; (VPD): vapour pressure deficit; (GR): global radiation; (RH): relative air humidity; (Tair): air temperature; (Tr): transpiration; (NEP): net ecosystem production: (SD): standard deviation.

Variable	Unit	Mean	SD	Range
NEP	μmol m^{-2} s^{-1}	12.1	9.2	-7.9 - 31.7
[O_3]	ppbv	42.9	11.2	12.0 - 79.5
FsO_3	nmol m^{-2} s^{-1}	8.3	3.6	0.072 - 17.6
GR	W m^{-2}	342.3	247.4	0.86 - 974
Tair	°C	17.7	6.1	1.3 - 33.8
RH	%	75.2	17.3	37.6 - 99.9
Tr	mm h^{-1}	0.0878	0.0754	0 - 0.37
VPD	kPa	0.624	0.585	0.0006 - 2.89

modification of g_{max} due to phenological changes, light intensity, air temperature, vapor pressure deficit, and soil water potential, respectively. g_{min} is the minimum FsO_3 that occurs during daylight hours.

The model was applied using environmental variables measured at the experimental station, although soil moisture deficit was estimated as a function of precipitation and daily mean surface temperature according to the principles of water budget. For more details and the site-specific model parameterisation see Zapletal et al. (2011).

Modelling and statistical analyses

The Generalized Additive Mixed Model (GAMM) was implemented in the "mgcv" package of the R ver. 3.4.0 program (Wood 2017) to assess the dependencies between NEP and its predictors GR, RH, Tair, VPD, and transpiration rate along with [O_3] and FsO_3 (Tab. 1). One-hour averages of all input data were used in GAMM. Only the data of the daytime period (06:00-18:00) when GR exceeded 10 W m^{-2} were used, so as to exclude periods where turbulence was not well-developed.

All predictors were tested and fitted by a

linear model, in the form of splines as smooth functions and as 1st degree linear interactions. Predictors were centred and, in the case of GR and RH, a square root transformation was used. Day of observation and autocorrelation pattern were tested as random factors. The best model was selected based on the AIC criteria and *p*-values. The model was started as one component containing all explanatory variables together with their interactions. By use of REML (Restricted Maximum Likelihood Estimation) the optimal structure of the random component was found. Then, optimal fixed structure using ML (Maximum Likehood) estimation was determined. Within the fixed structure, REML estimation was applied again.

Results

Microclimate conditions, [O_3] and FsO_3

The mean incoming daily sum of GR was 15.8 MJ m^{-2}, mean Tair was 15.03 °C, RH was 81.5%, and precipitation sum was 388 mm during the investigated period from May 28 to September 30. Soil volumetric water content remained high during the whole growing season ranging between 20 and
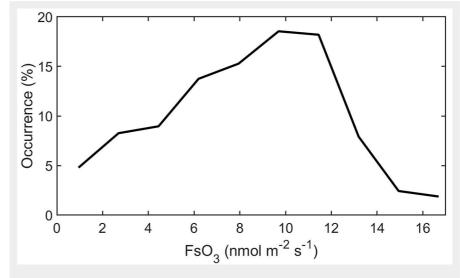

Fig. 2 - Relative occurrence of stomatal ozone flux (FsO_3) during the sunlight hours modelled for the period May 28-September 30, 2009.

Tab. 2 - Outputs of Generalized Additive Mixed Model (GAMM) predicting mixed effects of $[O_3]$ and other selected micrometeorological variables (predictors) on net ecosystem production (NEP). Linear predictors and linear interaction statistics are shown as *t*-values and *p*-values, whereas statistics of predictors used as smooth terms are shown as *F*-statistics, *p*-values and Edf. × indicate interaction. (Edf): estimated degree of freedom, Edf >1 indicate nonlinear relationships. R^2 (adjusted) = 0.948, n = 1440. $[O_3]$: ozone concentration; (VPD): vapour pressure deficit; (GR): global radiation; (RH): relative air humidity; (*Tair*): air temperature; (Tr): transpiration (***): $p<0.001$; (**): $p<0.01$; (*): $p<0.05$.

Predictor/ Interaction	Goodness of fit		Statistics		
	Parametric estimate	Edf	*t*-value	*F*	*p*-value
$[O_3]$	-0.042609	-	4.655	-	3.55e-06***
VPD	1.686854	-	2.226	-	0.026154*
$[O_3]$ × GR	-0.002573	-	-3.390	-	0.000717***
GR × RH	-0.100322	-	-6.310	-	3.73e-10***
GR × *Tair*	0.013316	-	6.919	-	6.84e-12***
GR × Tr	-0.476992	-	-3.499	-	0.000481***
VPD × GR	-0.280066	-	-8.314	-	<2e-16***
s(GR)	-	2.987	-	6835.670	<2e-16***
s(RH)	-	2.878	-	22.424	6.5e-13***
s(*Tair*)	-	2.4577	-	6.775	0.000807***
s(Tr)	-	2.384	-	5.168	0.003775**

Tab. 3 - Outputs of Generalized Additive Mixed Model (GAMM) predicting mixed effects of stomatal ozone flux (FsO_3) and other selected micrometeorological variables (predictors) on net ecosystem production (NEP). Linear predictors and linear interaction statistics are shown as *t*-values and *p*-values, whereas statistics of predictors used as smooth terms are shown as *F*-statistics, *p*-values and Edf. × indicate interaction. (Edf): estimated degree of freedom; Edf values >1 indicate nonlinear relationships. R^2 (adjusted) = 0.95, n = 1440. (FsO_3): stomatal ozone flux; (VPD): vapour pressure deficit; (GR): global radiation; (RH): relative air humidity; (*Tair*): air temperature; (Tr): transpiration; (***): $p<0.001$; (**): $p<0.01$; (*): $p<0.05$.
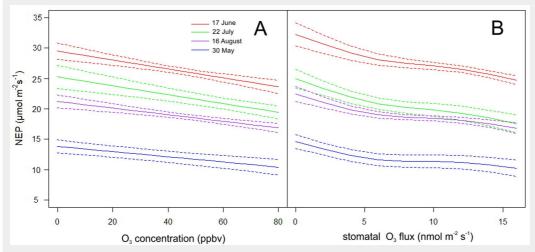
Predictor/ Interaction	Goodness of fit		Statistics		
	Parametric estimate	Edf	*t*-value	*F*	*p*-value
VPD	2.301725	-	2.850	-	0.00443**
GR × FsO_3	-0.016042	-	-4.577	-	5.14e-06***
GR × RH	-0.142519	-	-7.082	-	2.23e-12***
GR × *Tair*	0.014084	-	7.378	-	2.73e-13***
VPD × GR	-0.388303	-	-9.721	-	<2e-16***
s(GR)	-	2.973	-	6314.858	<2e-16***
s(RH)	-	2.865	-	18.079	5.99e-08***
s(*Tair*)	-	2.824	-	11.175	8.78e-07***
s(FsO_3)	-	2.933	-	22.547	7.77e-13***
s(Tr)	-	2.701	-	7.112	0.000131***

30% irrespective of actual sky conditions. Four model days, selected on the base of cloudiness degree (Fig. 1), represent (i) a sunny warm day with high *Tair* and VPD values (July 22) and (ii) partly-cloudy sky conditions with mild *Tair* and VPD (June 17 and August 16). (iii) The onset of the growing season (May 30) was characterized by the minimum values of GR, *Tair* and VPD. These days were also characterized by distinct $[O_3]$ with daily maxima ranging between 38 and 64 ppbv (Fig. 1D) as well as diurnal courses of FsO_3 (Fig. S1 in Supplementary material). The most frequent FsO_3 values ranged from 8-12 nmol m^{-2} s^{-1} during sunlight hours when the whole dataset is considered (Fig. 2).

GAMM outputs

The results of GAMM model for NEP prediction including $[O_3]$ and FsO_3 are shown in Tab. 2 and Tab. 3, respectively. Both models include a linear and non-linear part, as illustrated by the Edf parameter, which is presented only in the non-linear part. Only statistically significant predictors are shown. $[O_3]$ and VPD variables are shown only in Tab. 2, as their effect on NEP was only linear. Based on the Edf parameter, it was shown that FsO_3 had a non-linear effect on NEP (Tab. 3).

Statistically significant ($p < 0.01$) interactions were found between $[O_3]$ and GR and between FsO_3 and GR (Tab. 2, Tab. 3). Both interactions had negative values of parametric estimate (Tab. 2, Tab. 3) indicating that $[O_3]$ and FsO_3 led to a larger reduction of NEP with increasing GR. For example, natural FsO_3 led to a decrease in NEP by 1.07 µmol m^{-2} s^{-1}, comparing to pre-industrial era, at GR <300 W m^{-2}, whereas this reduction amounted up to 1.59 µmol m^{-2} s^{-1} (23.6%) at GR >500 W m^{-2}. The FsO_3 seems to be more tightly linked to ozone-induced decline of NEP than $[O_3]$ itself, based on explained variance by the models (R^2) and more significant *p*-value for FsO_3 ($p = 7.77e$-13) that $[O_3]$ ($p = 3.55e$-06). GR was identified as the most important driver of NEP, having the most significant *p* values (Tab. 2, Tab. 3).

Fig. 3 - Modelled relationships between net ecosystem production (NEP) and ozone concentration (A) and between NEP and stomatal ozone flux (B) for four representative days (full line). Models were applied with fixed predictors (see Tab. 1) measured at 11:00 of these representative days. Dashed lines represent the 95% confidence interval.

NEP modelling

NEP was predicted using $[O_3]$ (Fig. 3A) and FsO_3 (Fig. 3B) values in the range from zero to maximal values determined during the investigated growing season (May-September). Values of other predictors were fixed to values measured at 11:00 of the representative days. Both models predict a decrease in NEP with increasing $[O_3]$ or increasing FsO_3. Among the representative days, the highest decrease of NEP was found on May 30th, amounting to 21.6% (model run with $[O_3]$) and 30.4% (model run with FsO_3) when compared NEP at minimum (affected by 12 ppbv and 0.5 nmol m^{-2} s^{-1}) and maximum (affected by 80 ppbv and 17 nmol m^{-2} s^{-1}) values of $[O_3]$ and FsO_3, respectively. In July 22, the warmest month, the corresponding decreases were 24.9% and 28.9%. Diurnal courses of measured and modelled NEP during four representative days of the vegetation season are shown in Fig. 4.

Multi-factorial analysis (Fig. S2 in Supplementary material) revealed that high FsO_3 (17 nmol m^{-2} s^{-1}) has the most significant effect on NEP reduction in summer, while NEP decrease is driven more by GR than FsO_3 in spring and autumn. Moreover, VPD-induced stomatal closure was a main factor limiting NEP and stomatal O_3 flux in Norway spruce trees throughout the whole growing season. Therefore, a strong relationship between NEP reduction and stomatal conductance, not only the simple $[O_3]$ outside the leaves, can be suggested.

Taking to the account the whole dataset, the GAMM based calculated NEP was higher by up to 12.4% at low, preindustrial ozone concentration (12 ppbv) as compared to the measured NEP at the present concentration of 42.9 ± 11.2 ppbv (mean ± SD – Tab. 1). Similarly, the GAMM based on
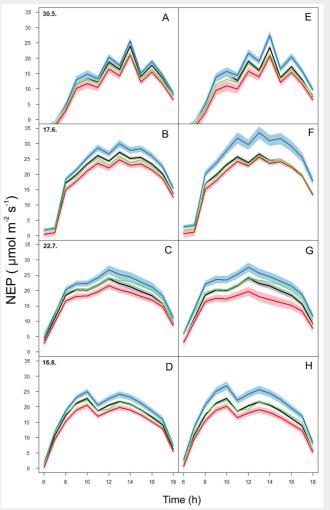

Fig. 4 - Predicted diurnal courses of net ecosystem production (NEP) using Generalized Additive Mixed Model with ozone concentration (O_3, A,B,C,D) and stomatal ozone flux (FsO_3, E,F,G,H). Three levels of O_3 and FsO_3 were used to predict NEP: Blue line - low O_3 (10 ppbv) and FsO_3 (0.5 nmol m^{-2} s^{-1}), red line - high O_3 (80 ppbv) and FsO_3 (17 nmol m^{-2} s^{-1}), and black line - actual, measured O_3 and FsO_3. Green line represents NEP measured by an eddy covariance system. Shaded area represents prediction bounds at 95% confidence level.

FsO_3 revealed NEP to be elevated by up to 24.8% under the condition of low FsO_3 (0.5 nmol m^{-2} s^{-1}) as compared to actual FsO_3 of 8.3 ± 3.7 nmol m^{-2} s^{-1} (mean ± SD). In contrast, high $[O_3]$ (80 ppbv) and high FsO_3 (17 nmol m^{-2} s^{-1}) were found to lead to a decrease in NEP by 24% and 38.9%, respectively as compared to preindustrial NEP val-

Tab. 4 - Mean values of ambient (Amb) ozone concentration ($[O_3]$; ppbv) and stomatal ozone flux (FsO_3; nmol m^{-2} s^{-1}), and Net ecosystem production (NEP; μmol m^{-2} s^{-1}) predicted by a Generalized Additive Mixed Model for the conditions of actual (measured), high, and low $[O_3]$ and FsO_3 during the individual months of the growing season and the whole dataset covering May 28-September 30, 2009. Δ represents percentage difference of predicted NEP to mean NEP measured by an eddy covariance system. (a) values of Δ represent percentage decrease in NEP induced by high O_3 (80 ppbv) and/or FsO_3 (17 nmol m^{-2} s^{-1}); (b): values of Δ represent percentage increase in NEP at low O_3 (12 ppbv) and/or FsO_3 (0.5 nmol m^{-2} s^{-1}).

Months	Conditions	Amb $[O_3]$	Low $[O_3]$	High $[O_3]$	Amb FsO_3	Low FsO_3	High FsO_3
May	$[O_3]$/FsO_3	36.5	12	80	5.5	0.5	17
	NEP	7.9	9.6	7.2	7.9	10.8	7.2
	Δ	-	21.5 [b]	8.9 [a]	-	36.7 [b]	8.9 [a]
June	$[O_3]$/FsO_3	42	12	80	9.1	0.5	17
	NEP	10.2	12.5	9.7	10.2	14.1	7.7
	Δ	-	22.5 [b]	4.9 [a]	-	38.2 [b]	24.5 [a]
July	$[O_3]$/FsO_3	46.2	12	80	8.98	0.5	17
	NEP	15.3	17.2	13.8	15.3	18.7	13.5
	Δ	-	12.4 [b]	9.8 [a]	-	22.2 [b]	11.8 [a]
Aug	$[O_3]$/FsO_3	45	12	80	8.5	0.5	17
	NEP	12.6	13.9	11	12.6	15.4	10.9
	Δ	-	10.3 [b]	12.7 [a]	-	22.2 [b]	13.5 [a]
Sept	$[O_3]$/FsO_3	39.1	12	80	7.2	0.5	17
	NEP	10.4	10.8	8.3	10.4	12.3	8.5
	Δ	-	3.8	20.2	-	18.3	18.3
Whole dataset	$[O_3]$/FsO_3	42.9	12	80	8.3	0.5	17
	NEP	12.1	13.6	10.7	12.1	15.1	10.4
	Δ	-	12.4	11.6	-	24.8	14.1

ues which were unaffected by high [O_3] and/or FsO_3 (Tab. 4).

In addition, we present estimated changes in NEP under the conditions of low/high [O_3] and FsO_3 during individual months of the growing season (May-September – Tab. 4). Both models confirmed a high percentage reduction of NEP occurring in spring (May-June), comparing values of current NEP to preindustrial ones, while the O_3-induced NEP reduction in September was relatively small. The largest absolute reduction occurred, however, in June and July when NEP reaches a seasonal maximum. Contrary to those findings, the largest percentage and absolute NEP reductions predicted at high [O_3] and FsO_3 were found in September whereas the lowest ones in June.

Discussion

Projections of O_3-induced damage are uncertain due to numerous scenarios dealing with different future [O_3] or FsO_3. Ozone in the Northern Hemisphere is projected to increase further by 20-25% between 2015 and 2050, and by 40-60% by 2100, if current ozone-precursors (CO_2, volatile organic compounds, NO_x) emission trends continue (Meehl et al. 2007). Sitch et al. (2007) projected a decrease in NEP by 14-23% over the period 1901-2100 owing to plant damage caused by [O_3] with regional reduction peeking up to 30%. However, recent studies suggest [O_3] decreases on average by 0-2 ppbv between 2000-2030 years, rising to 10 ppbv in 2100 in north latitudes (Young et al. 2013). Those findings are in accordance with Klingberg et al. (2014), who expected a decrease of O_3 precursors, particularly biogenic volatile organic compounds (BVOCs) and nitrogen oxides (NO_x), according to RCP4.5 scenario, which should consequently lead to decrease of European vegetation damage. However, extreme periods expected under future climate conditions may lead to episodes with high [O_3]. For example, severe drought conditions in 2003 were associated with high [O_3] in the Central Europe (Solberg et al. 2008). In relation to regional climate, Beniston (2004) assumed that the year 2003 could be used as an analogy of future dry summer seasons resulting in high emissions of BVOCs and NO_x (Young et al. 2013), which showed to depend highly on season also at Bílý Kríž (Juráň et al. 2017). Future impacts on ozone concentration across Europe show contradicting results: under RCP8.5 scenario, [O_3] of temperate coniferous forest could increase by 10.2 ppbv as modelled for coniferous forests at Hengduan Shan, China forests (Fuhrer et al. 2016). On the other hand, a modelling study for the temperate coniferous forest of the Sierra Nevada suggests a decrease in [O_3] by 6 ppbv from 2000 to 2050 (Fuhrer et al. 2016) in accordance with the [O_3] decrease by 5 ppbv per decade (Cooper et al. 2014). In our study we have contrasted the O_3 effects on NEP at low, pre-industrial [O_3] of

12 ppbv and high [O_3] of 80 ppbv.

Numerous studies have shown that elevated [O_3] generally results in reduced photosynthesis, chlorophyll content and whole-plant growth, decreased stomatal conductance, an altered antioxidant system, accelerated senescence and changes the plant metabolism, although the extent of the effects varies by species, length of exposure, [O_3] and/or co-occurrence of other stress factors (reviewed in Wallin et al. 2002, Kontunen-Soppela et al. 2007, Hoshika et al. 2018). In accordance with these studies we have found here that both increasing [O_3] and FsO_3 significantly reduced NEP of mature Norway spruce forest grown under natural mountain conditions (Fig. 3). Moreover, our analyses show that the use of FsO_3 provides an improved fit to NEP experimental data as compared to the predictions of a merely [O_3]-based GAMM model, particularly under hot summer days (Tab. 4). Differences between the measured and predicted NEP by the model with [O_3] and FsO_3 expressed as a model error amounted to 0.41% and 0.17%, respectively. The theory behind this is that stomata substantially regulate both CO_2 and O_3 diffusion into the leaf interior leading thus to a modulation of photosynthetic activity and the magnitude of O_3-induced injuries, respectively. We assume that stomata remain open under the conditions of low VPD and sufficient light intensity (Urban et al. 2012). Accordingly, high FsO_3 can be expected though ambient [O_3] is relatively low and can lead to a substantial NEP reduction. On the contrary, conditions of high VPD and/or high temperature may result in a marked closure of stomata. While an ambient [O_3] is usually high under such conditions, O_3-induced reduction of NEP may be depressed due to a low FsO_3 into a leaf interior. Therefore, models with high FsO_3 may predict higher reduction in NEP than models with high [O_3] (Fig. 3). Such results imply that not only high [O_3], but particularly high FsO_3 induces injuries on vegetation and reduces carbon assimilation (Matyssek et al. 2007, Fares et al. 2013).

We predicted higher NEP (by 24.6% on average) at low FsO_3 of 0.5 nmol m^{-2} s^{-1} as compared to NEP at current FsO_3 of 8.32 ± 3.66 nmol m^{-2} s^{-1} with the highest absolute reduction occurring in June and July (Tab. 4). Karlsson (2012) stated that reduction of the living biomass carbon stock caused by the ozone problem among the Central and Northern European countries ranges from 2% (Norway, Finland) to 32% in the Czech Republic, when compared to the pre-industrial age. Satellite data over the European continent suggest a decline of photosynthetic carbon uptake ranging between 0.4-30% due to O_3 damage depending on the forest type and location. Highest negative effects of O_3 were found in coniferous forests (Proietti et al. 2016). Moreover, these authors identified air temperature, soil water content, and relative air humidity as key predictors of NEP describing more than 81%

of NEP variability. Soil water content was, however, omitted into our model, since soil water content was not a limiting factor in our case study under the wet mountainous conditions. However, air temperature and relative air humidity (ultimately VPD), play significant roles in our model together with GR. Similarly to our findings, Anav et al. (2011) reported a reduction of photosynthetic carbon uptake per day caused by [O_3] of about 22% in boreal and temperate forests. FACE fumigation experiment of enhanced CO_2 and [O_3] on temperate forest dominated by *Betula papyrifera* Marsh. and *Acer saccharum* Marsh. in USA revealed reduction of cumulative net primary productivity of 9% (Talhelm et al. 2014). However, Finco et al. (2017) estimated relatively low decreases in biomass production by 4-5 % in Alpine larch forest caused by current [O_3] when compared to the pre-industrial era, even if the total ozone fluxes were generally high, up to 30-40 nmol m^{-2} s^{-1}. This was due to relatively low portion of stomatal uptake by the larch forest representing only 15-16% of total O_3 deposition flux into the forest. Similar growth reductions in stem increment of 6.6% and photosynthetic carbon uptake of 4-8% were observed in Switzerland (Braun et al. 2014) and eastern parts of USA (Yue & Unger 2014), respectively, due to episodes of high tropospheric [O_3].

Norway spruce, one of the most common and important timber trees in Europe, was found to be an O_3 sensitive tree species, showing substantial reductions in photosynthetic carbon uptake under elevated [O_3] (Wallin et al. 2002, Zapletal et al. 2011). For example, Subramanian et al. (2015) reported a decrease in carbon sequestration of spruce forest in Sweden by 4.3-15.5% under ambient ozone conditions as compared to the preindustrial [O_3]. This is consistent with our estimate of NEP reduction in mountain spruce forest of the temperate zone.

It should be noted, however, that there is a contrasting evidence of long-term O_3 effects detected after several growing seasons. Since several research groups reported no negative effect of elevated [O_3] on carbon assimilation in forest ecosystems (Zak et al. 2011, Wang et al. 2016), we can hypothesize large acclimation capacity of tree species, including morphological (Riikonen et al. 2004, 2010) as well as biochemical adjustments (reviewed by Heath 2008). Recent studies have, however, shown that long-term exposure to elevated [O_3] may substantially modulate an acclimation of trees to other environmental factors like elevated temperature (Kivimäenpää et al. 2017) and/or elevated atmospheric CO_2 concentration (Riikonen et al. 2010, Zak et al. 2011). The carbon sink strength in old forests could be thus reduced substantially or even disappear under the conditions of high [O_3], accelerating the impact of atmospheric CO_2 on climate change. Precise estimates of FsO_3 are

thus needed for future predictions of ozone impacts on NEP of terrestrial ecosystems.

Conclusions

We have found that stomatal ozone flux model tracks diurnal changes in NEP more precisely that ozone concentration model does. NEP simulated at low, pre-industrial FsO_3 (0.5 nmol m^{-2} s^{-1}) was higher by 24.8% as compared to NEP assessed at current FsO_3 (8.32 nmol m^{-2} s^{-1}). Further increase in FsO_3 (up to 17 nmol m^{-2} s^{-1}) may lead to subsequent reduction in NEP by 14.1% in average as compared to current NEP values, but this reduction may change during the growing season. These results are in agreement with observations in other European coniferous forests. Relatively high site-specific variability in $[O_3]$ effect of photosynthetic carbon uptake is likely caused by species-specific sensitivity of stomata to environmental drivers. Also a co-occurrence of other stress factors, particularly extreme temperatures and drought, leading to the changes in stomatal conductance and stomatal ozone flux, may influence a final response of trees to $[O_3]$.

Acknowledgement

References

Anav A, Menut L, Khvorostyanov D, Viovy N (2011). Impact of tropospheric ozone on the Euro-Mediterranean vegetation. Global Change Biology 17: 2342-2359. - doi: 10.1111/j.1365-2486.2010.02387.x

Andersen CP (2003). Source-sink balance and carbon allocation below ground in plants exposed to ozone. New Phytologist 157: 213-228. - doi: 10.1046/j.1469-8137.2003.00674.x

Aubinet M, Vesala T, Papale D (2012). Eddy Covariance. Springer, Dordrecht-Heidelberg-London-New York, pp. 438. - doi: 10.1007/978-94-007-2351-1

Beniston M (2004). The 2003 heat wave in Europe: a shape of things to come? An analysis based on Swiss climatological data and model simulations. Geophysical Research Letters 31: L02202. - doi: 10.1029/2003GL018857

Braun S, Schindler C, Rihm B (2014). Growth losses in Swiss forests caused by ozone: Epidemiological data analysis of stem increment of *Fagus sylvatica* L. and *Picea abies* Karst. Environmental Pollution 192: 129-138. - doi: 10.1016/j.envpol.2014.05.016

Cieslik S (2004). Ozone uptake by various surface types: a comparison between dose and exposure. Atmospheric Environment 38: 2409-2420. - doi: 10.1016/j.atmosenv.2003.10.063

Cooper OR, Parrish DD, Ziemke J, Balashov NV, Cupeiro M, Galbally IE, Gilge S, Horowitz L, Jensen NR, Lamarque J-F, Naik V, Oltmans SJ, Schwab J, Shindell DT, Thompson AM, Thouret V, Wang Y, Zbinden RM (2014). Global distribution and trends of tropospheric ozone: an observation-based review. Elementa 2: 000029. - doi: 10.12952/journal.elementa.000029

Emberson LD, Ashmore MR, Cambridge H, Simpson D, Tuovinen J-P (2000). Modelling stomatal ozone flux across Europe. Environmental Pollution 109: 403-414. - doi: 10.1016/S0269-7491(00)00043-9

Fares S, Vargas R, Detto M, Goldstein AH, Karlik J, Paoletti E, Vitale M (2013). Tropospheric ozone reduces carbon assimilation in trees: estimates from analysis of continuous flux measurements. Global Change Biology 19: 2427-2443. - doi: 10.1111/gcb.12222

Fares S, Conte A, Chabbi A (2018). Ozone flux in plant ecosystems: new opportunities for long-term monitoring networks to deliver ozone-risk assessments. Environmental Science and Pollution Research 25: 8240-8248. - doi: 10.1007/s11356-017-0352-0

Finco A, Marzuoli R, Chiesa M, Gerosa G (2017). Ozone risk assessment for an Alpine larch forest in two vegetative seasons with different approaches: comparison of POD1 and AOT40. Environmental Science and Pollution Research 24: 26238-26248. - doi: 10.1007/s11356-017-9301-1

Fuhrer J, Val Martin M, Mills G, Heald CL, Harmens H, Hayes F, Sharps K, Bender J, Ashmore MR (2016). Current and future ozone risks to global terrestrial biodiversity and ecosystem processes. Ecology and Evolution 6: 8785-8799. - doi: 10.1002/ece3.2568

Heath RL (2008). Modification of the biochemical pathways of plants induced by ozone: what are the varied routes to change? Environmental Pollution 155: 453-463. - doi: 10.1016/j.envpol.2008.03.010

Hoshika Y, Watanabe M, Carrari E, Paoletti E, Koike T (2018). Ozone-induced stomatal sluggishness changes stomatal parameters of Jarvis-type model in white birch and deciduous oak. Plant Biology 20: 20-28. - doi: 10.1111/plb.12632

Juráň S, Pallozzi E, Guidolotti G, Fares S, Šigut L, Calfapietra C, Alivernini A, Savi F, Večeřová K, Křůmal K, Večeřa Z, Urban O (2017). Fluxes of biogenic volatile organic compounds above temperate Norway spruce forest of the Czech Republic. Agricultural and Forest Meteorology 232: 500-513. - doi: 10.1016/j.agrformet.2016.10.005

Karlsson PE (2012). Ozone impacts on carbon sequestration in northern and central European forests. IVL Report B 2065, IVL Swedish Environmental Research Institute, Gothenburg, Sweden, pp. 25. [online] URL: http://icpvegetation.ceh.ac.uk/events/documents/Karlsson.pdf

Kivimäenpää M, Sutinen S, Valolahti H, Häikiö E, Riikonen J, Kasurinen A, Ghimire RP, Holopainen JK, Holopainen T (2017). Warming and elevated ozone differently modify needle anatomy of Norway spruce (*Picea abies*) and scots pine (*Pinus sylvestris*). Canadian Journal of Forest Research 47: 488-499. doi: 10.1139/cjfr-2016-0406

Klingberg J, Engardt M, Karlsson PE, Langner J, Pleijel H (2014). Declining ozone exposure of European vegetation. Biogeosciences 11: 5269-5283. - doi: 10.5194/bg-11-5269-2014

Kontunen-Soppela S, Ossipov V, Ossipova S, Oksanen E (2007). Shift in birch leaf metabolome and carbon allocation during long-term open field ozone exposure. Global Change Biology 13: 1053-1067. - doi: 10.1111/j.1365-2486.2007.01332.x

Matyssek R, Bytnerowicz A, Karlsson P-E, Paoletti E, Sanz M, Schaub M, Wieser G (2007). Promoting the O_3 flux concept for European forest trees. Environmental Pollution 146: 587-607. - doi: 10.1016/j.envpol.2006.11.011

Meehl GA, Covey C, Delworth T, Latif M, McAvaney B, Mitchell JFB, Stouffer RJ, Taylor KE (2007). The WCRP CMIP3 multimodel dataset. Bulletin of the American Meteorological Society 88: 1383-1394. - doi: 10.1175/BAMS-88-9-1383

Musselman RC, Massman WJ (1998). Ozone flux to vegetation and its relationship to plant response and ambient air quality standards. Atmospheric Environment 33: 65-73. - doi: 10.1016/S1352-2310(98)00127-7

Paoletti E, De Marco A, Beddows DCS, Harrison RM, Manning WJ (2014). Ozone levels in European and USA cities are increasing more than at rural sites, while peak values are decreasing. Environmental Pollution 192: 295-299. - doi: 10.1016/j.envpol.2014.04.040

Proietti C, Anav A, De Marco A (2016). A multi-sites analysis on the ozone effects on Gross Primary Production of European forests. Science of the Total Environment 556: 1-11. - doi: 10.1016/j.scitotenv.2016.02.187

Reichstein M, Falge E, Baldocchi D, Papale D, Aubinet M, Berbigier P, Bernhofer C, Buchmann N, Gilmanov T, Granier A, Grünwald T, Havránková K, Ilvesniemi H, Janous D, Knohl A, Laila T, Lohila A, Loustau D, Matteucci G, Meyers T, Miglietta F, Ourcival JM, Pumpanen J, Rambal S, Rotenberg E, Sanz M, Tenhunen J, Seufert G, Vaccari F (2005). On the separation of net ecosystem exchange into assimilation and ecosystem respiration: review and improved algorithm. Global Change Biology 11: 1424-1439. - doi: 10.1111/j.1365-2486.2005.001002.x

Riikonen J, Lindsberg MM, Holopainen T, Oksanen E, Lappi J, Peltonen P, Vaavouri E (2004). Silver birch and climate change: variable growth and carbon allocation responses to elevated concentration of carbon dioxide and ozone. Tree Physiology 24: 1227-1237. - doi: 10.1093/treephys/24.11.1227

Riikonen J, Percy KE, Kivimäenpää M, Kubiske ME, Nelson ND, Vapaavouri E, Karnosky DF (2010). Leaf size and surface characteristics of *Betula papyrifera* exposed to elevated CO_2 and O_3. Environmental Pollution 158: 1029-1035. - doi: 10.1016/j.envpol.2009.07.034

Royal Society (2008). Ground-level ozone in the 21st century: future trends, impacts and policy implications. The Royal Society, London, UK, pp. 132.

Samuelson LJ (1994). Ozone-exposure responses of black cherry and red maple seedlings. Environmental and Experimental Botany 34: 355-362. - doi: 10.1016/0098-8472(94)90017-5

Sicard P, Augustaitis A, Belyazid S, Calfapietra C, DeMarco A, Fenn M, Grulke N, He S, Matyssek R, Serengil Y, Wieser G, Paoletti E (2016). Global topics and novel approaches in the study of air pollution, climate change and forest ecosys-

tems. Environmental Pollution 213: 977-987. - doi: 10.1016/j.envpol.2016.01.075

Sitch S, Cox PM, Collins WJ, Huntingford C (2007). Indirect radiative forcing of climate change through ozone effects on the land-carbon sink. Nature 448: 791-794. - doi: 10.1038/nature06059

Skärby L, Ro-Poulsen H, Wellburn FAM, Sheppard LJ (1998). Impacts of ozone on forests: a European perspective. New Phytologist 139: 109-122. - doi: 10.1046/j.1469-8137.1998.00184.x

Solberg S, Hov O, Sovde A, Isaksen ISA, Coddeville P, De Backer H, Forster C, Orsolini Y, Uhse K (2008). European surface ozone in the extreme summer 2003. Journal of Geophysical Research Atmospheres 113: D07307. - doi: 10.1029/2007JD009098

Subramanian N, Karlsson PE, Bergh J, Nilsson U (2015). Impact of ozone on sequestration of carbon by Swedish forests under a changing climate: a modeling study. Forest Science 61: 445-457. - doi: 10.5849/forsci.14-026

Sun G, McLaughlin SB, Porter JH, Uddling J, Mulholland PJ, Adams MB, Pederson N (2012). Interactive influences of ozone and climate on streamflow of forested watersheds. Global Change Biology 18: 3395-3409. - doi: 10.1111/j.1365-2486.2012.02787.x

Talhelm AF, Pregitzer KS, Kubiske ME, Zak DR, Campany CE, Burton AJ, Dickson RE, Hendrey GR, Isebrands JG, Lewin KF, Nagy J, Karnosky DF (2014). Elevated carbon dioxide and ozone alter productivity and ecosystem carbon content in northern temperate forests. Global Change Biology 20: 2492-2504. - doi: 10.1111/gcb.12564

Urban O, Klem K, Ač A, Havránková K, Holišová P, Navrátil M, Zitová M, Kozlová K, Pokorný R, Šprtová M, Tomášková I, Špunda V, Grace J (2012). Impact of clear and cloudy sky conditions on the vertical distribution of photosynthetic CO_2 uptake within a spruce canopy. Functional Ecology 26: 46-55. - doi: 10.1111/j.1365-2435.2011.01934.x

Verryckt LT, Op De Beeck M, Neirynck J, Gielen B, Roland M, Janssens IA (2017). No impact of tropospheric ozone on the gross primary productivity of a Belgian pine forest. Biogeosciences 14: 1839-1855. - doi: 10.5194/bg-14-1839-2017

Wallin G, Karlsson PE, Selldén G, Ottosson S, Medin EL, Pleijel H, Skärby L (2002). Impact of four years exposure to different levels of ozone, phosphorus and drought on chlorophyll, mineral nutrients, and stem volume of Norway spruce, *Picea abies*. Physiologia Plantarum 114: 192-206. - doi: 10.1034/j.1399-3054.2002.1140205.x

Wang B, Shugart HH, Shuman JK, Lerdau MT (2016). Forests and ozone: productivity, carbon storage, and feedbacks. Scientific Reports 6: 22133. - doi: 10.1038/srep22133

Wittig VE, Ainsworth EA, Naidu SL, Karnosky DF, Long SP (2009). Quantifying the impact of current and future tropospheric ozone on tree biomass, growth, physiology and biochemistry: a quantitative meta-analysis. Global Change Biology 15: 396-424. - doi: 10.1111/j.1365-2486.2008.01774.x

Wood SN (2017). Generalized additive models: an introduction with R (2nd edn). Chapman and Hall/CRC, New York, USA, pp. 476. [online] URL: http://www.taylorfrancis.com/books/9781498728348

Young PJ, Archibald AT, Bowman KW, Lamarque JF, Naik V, Stevenson DS, Tilmes S, Voulgarakis A, Wild O, Bergmann D, Cameron-Smith P, Cionni I, Collins WJ, Dalsren SB, Doherty RM, Eyring V, Faluvegi G, Horowitz LW, Josse B, Lee YH, MacKenzie IA, Nagashima T, Plummer DA, Righi M, Rumbold ST, Skeie RB, Shindell DT, Strode SA, Sudo K, Szopa S, Zeng G (2013). Preindustrial to end 21st century projections of tropospheric ozone from the Atmospheric Chemistry and Climate Model Intercomparison Project (ACCMIP). Atmospheric Chemistry and Physics 13: 2063-2090. - doi: 10.5194/acp-13-2063-2013

Yue X, Keenan TF, Munger W, Unger N (2016). Limited effect of ozone reductions on the 20-year photosynthesis trend at Harvard forest. Global Change Biology 22: 3750-3759. - doi: 10.1111/gcb.13300

Yue X, Unger N (2014). Ozone vegetation damage effects on gross primary productivity in the United States. Atmospheric Chemistry and Physics 14: 9137-9153. - doi: 10.5194/acp-14-9137-2014

Zak DR, Pregitzer KS, Kubiske ME, Burton AJ (2011). Forest productivity under elevated CO_2 and O_3: positive feedbacks to soil N cycling sustain decade-long net primary productivity enhancement by CO_2. Ecology Letters 14: 1220-1226. - doi: 10.1111/j.1461-0248.2011.01692.x

Zapletal M, Cudlín P, Chroust P, Urban O, Pokorný R, Edwards-Jonášová M, Czerný R, Janouš D, Taufarová K, Večeřa Z, Mikuška P, Paoletti E (2011). Ozone flux over a Norway spruce forest and correlation with net ecosystem production. Environmental Pollution 159: 1024-1034. - doi: 10.1016/j.envpol.2010.11.037

Zapletal M, Pretel J, Chroust P, Cudlín P, Edwards-Jonášová M, Urban O, Pokorný R, Czerný R, Hůnová I I (2012). The influence of climate change on stomatal ozone flux to a mountain Norway spruce forest. Environmental Pollution 169: 267-273. - doi: 10.1016/j.envpol.2012.05.008

Zona D, Gioli B, Fares S, De Groote T, Pilegaard K, Ibrom A, Ceulemans R (2014). Environmental controls on ozone fluxes in a poplar plantation in Western Europe. Environmental Pollution 184: 201-210. - doi: 10.1016/j.envpol.2013.08.032

Supplementary Material

Fig. S1 - Diurnal courses of modelled stomatal ozone flux (FsO_3) in Norway spruce forest during the investigated period of May 28 - September 30, 2009.

Fig. S2 - Principal component analysis revealing dependencies of environmental variables among each other.

Link: Juran_2805@suppl001.pdf